



SST–North American Hydroclimate Links in AMIP Simulations of the Drought Working Group Models: A Proxy for the Idealized Drought Modeling Experiments

ALFREDO RUIZ-BARRADAS

Department of Atmospheric and Oceanic Science, University of Maryland, College Park, College Park, Maryland

SUMANT NIGAM

Department of Atmospheric and Oceanic Science, and Earth System Science Interdisciplinary Center, University of Maryland, College Park, College Park, Maryland

(Manuscript received 1 April 2009, in final form 23 December 2009)

ABSTRACT

The present study assesses the potential of the U.S. Climate Variability and Predictability (CLIVAR) Drought Working Group (DWG) models in simulating interannual precipitation variability over North America, especially the Great Plains. It also provides targets for the idealized DWG model experiments investigating drought origin. The century-long Atmospheric Model Intercomparison Project (AMIP) simulations produced by version 3.5 of NCAR's Community Atmosphere Model (CAM3.5), the Lamont-Doherty Earth Observatory's Community Climate Model (CCM3), and NASA's Seasonal-to-Interannual Prediction Project (NSIPP-1) atmospheric models are analyzed; CCM3 and NSIPP-1 models have 16- and 14-ensemble simulations, respectively, while CAM3.5 only has 1.

The standard deviation of summer precipitation is different in AMIP simulations. The maximum over the central United States seen in observations is placed farther to the west in simulations. Over the central plains the models exhibit modest skill in simulating low-frequency precipitation variability, a Palmer drought severity index proxy. The presence of a linear trend increases correlations in the period 1950–99 when compared with those for the whole century. The SST links of the Great Plains drought index have features in common with observations over both the Pacific and Atlantic Oceans.

Interestingly, summer-to-fall precipitation regressions of the *warm Trend*, *cold Pacific*, and *warm Atlantic* modes of annual mean SST variability (used in forcing the DWG idealized model experiments) tend to dry the southwestern, midwestern, and southeastern regions of the United States in the observations and, to a lesser extent, in the simulations.

The similarity of the idealized SST-forced droughts in DWG modeling experiments with AMIP precipitation regressions of the corresponding SST principal components, evident especially in the case of the cold Pacific pattern, suggests that the routinely conducted AMIP simulations could have served as an effective proxy for the more elaborated suite of DWG modeling experiments.

1. Introduction

The U.S. Climate Variability and Predictability (CLIVAR) Drought Working Group (DWG) has been leading the national efforts toward a better understanding of multiyear droughts for the past two and a half years.

The main objective of the group has been to facilitate progress on the understanding and prediction of long-term multiyear droughts over North America and other drought-prone regions of the world, including an assessment of the impact of global change on drought processes (Gutzler and Schubert 2007). In this task, a central idea has been for several modeling groups to do identical idealized experiments to look in detail at the physical mechanisms linking SST changes to droughts.

In a nutshell, there are five research centers, with their respective state-of-the-art atmospheric GCMs, that

Corresponding author address: Alfredo Ruiz-Barradas, 3435 Computer and Space Sciences Bldg., University of Maryland, College Park, College Park, MD 20742-2425.
E-mail: alfredo@atmos.umd.edu

participate in the idealized experiments: 1) the National Center for Atmospheric Research's (NCAR) Community Atmosphere Model, version 3.5 (CAM3.5) (Neale et al. 2008; Oleson et al. 2008); 2) NCAR's Community Climate Model (CCM3) run by the Lamont-Doherty Earth Observatory group (Kiehl et al. 1998; Seager et al. 2005); 3) the National Aeronautics and Space Administration Geophysical Fluid Dynamics Laboratory (NASA GSFC) Seasonal-to-Interannual Prediction Project (NSIPP-1) model (Bacmeister et al. 2000; Schubert et al. 2004); 4) the NOAA-National Centers for Environmental Prediction's (NCEP) Global Forecasting System (GFS) model (Campana and Caplan 2009); and 5) the Geophysical Fluid Dynamics Laboratory (NOAA/GFDL) Atmospheric Model (AM2.1) (Delworth et al. 2006). The main drought experiments are carried out by superposing specific SST anomaly patterns set in time on monthly varying SST climatology. There are three main SST anomaly patterns with distinct structures that can be linked to Trend, Pacific, and Atlantic modes of annual-mean SST variability (Fig. 1). In the companion paper by Schubert et al. (2009), details about these experiments are given, namely, the models used, the SST forcing, and an overview of the results.

The hierarchy of interactions that give rise to precipitation variability within a model, that is, local land surface-atmosphere versus remote SST-moisture fluxes, plays a crucial role in the simulation of regional summer hydroclimate variability. Regional hydroclimate over the central United States strongly depends on the moisture transport from the Gulf of Mexico via the Great Plains low-level jet, particularly in the summer season (e.g., Ruiz-Barradas and Nigam 2005, 2006a; Weaver and Nigam 2008). However, some of the state-of-the-art models prioritize local land surface-atmosphere interactions over remote SST-moisture flux convergence interactions at interannual-to-larger scales, which are at odds with observations (Ruiz-Barradas and Nigam 2005, 2006b). In spite of the dominance of the local interactions in those models, links between summer precipitation variability at low frequencies and SSTs are still present (Ruiz-Barradas and Nigam 2009, manuscript submitted to *J. Climate*). Several other studies have documented the importance of the SST links of the central U.S. hydroclimate (e.g., Trenberth and Guillemot 1996; Ting and Wang 1997; Barlow et al. 2001; Schubert et al. 2004).

The main goal of the current study is to document, and to assess, the capabilities of the DWG atmospheric models in simulating low-frequency summer precipitation variability over North America from century-long Atmospheric Model Intercomparison Project (AMIP) simulations. Emphasis is on establishing 1) SST links of Great Plains low-frequency summer precipitation and 2)

seasonality and structure of the responses of precipitation to the modes of annual-mean SST variability that force the idealized drought simulations. The precipitation-centric analysis of Great Plains low-frequency summer precipitation variability in the models forced by observed SSTs allows us to explore to what extent that variability is linked to anomalous SSTs in the models and establish the basis for the SST-centric analysis of the impact of the annual-mean SST modes on the regional precipitation variability. The present paper focuses on the available AMIP simulations, associated with the models used for the idealized experiments, and their potential to be used as an alternative to the idealized experiments. Although there are five models reporting results for the idealized experiments, only simulations with CAM3.5, CCM3, and NSIPP-1 will be analyzed because the NCEP's AMIP simulations are very short for the present study and NOAA/GFDL has not made public its AMIP simulations.

The paper is organized beginning with section 2, which provides some basic information on the models and their simulations as well as the observational data. Next, in section 3 the interannual variability of summer precipitation in North America in general, and in the Great Plains in particular, is analyzed. Then, section 4 elaborates on the SST links of summer precipitation variability in the Great Plains. Section 5 provides seasonal precipitation targets over North America for the idealized experiments. In section 6 one idealized experiment is compared with one of the regression targets. Finally, the paper ends with section 7, which summarizes the main conclusions.

2. Datasets

As mentioned in the introduction, the present analysis will focus on century-long simulations. Thus, only three of the models will be analyzed: CAM3.5, CCM3, and NSIPP-1. Details of the models, their SST forcing, and the AMIP runs are summarized in Table 1. While the CAM3.5 model only provides one single simulation, the CCM3 and NSIPP-1 models provide sets of 16 and 14 simulations. Calculations are performed for each ensemble member from the CCM3 and NSIPP-1 models, and then the mean of a given calculation is displayed.

A small number of observed datasets are employed. An observational target for the simulated precipitation is given by the CRUTS2.1 precipitation dataset of the University of East Anglia's Climate Research Unit (CRU) (Mitchell 2005). The dataset is on a 0.5° grid for the land areas of the globe and spans the time period from 1901 through 2002. The global Palmer drought severity index (PDSI) is also used, but only as an area-averaged index; the dataset is on a 2.5° grid at monthly resolution for the time period 1870–2003 (Dai et al. 2004).

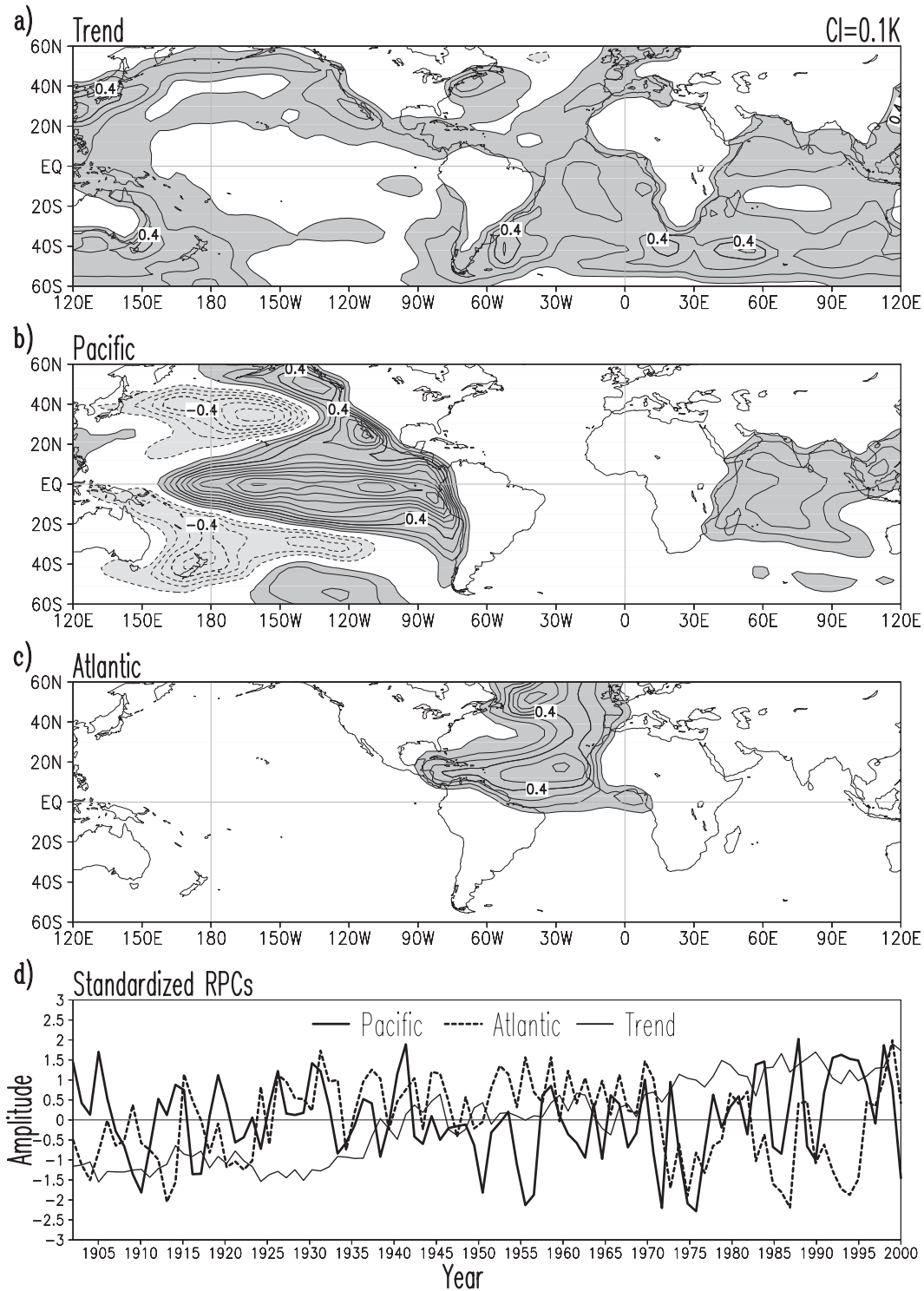


FIG. 1. Main modes of annual-mean SST variability calculated for the period 1901–2004. Modes were obtained by a rotated EOF analysis. The SST anomalies for the (a) Trend, (b) Pacific, and (c) Atlantic modes have been used in the idealized experiments lead by the U.S. CLIVAR DWG (Schubert et al. 2009). Positive (negative) anomalies are shaded dark (light). The contour interval is 0.1 K and shading is used for values ≥ 0.1 K. Anomalies have been smoothed with the Grid Analysis and Display System (GrADS) function smth9. (d) Associated rotated PCs standardized for the 1902–99 period to be used in the current study are shown; standardization was made by subtracting the mean anomaly and then dividing by the standard deviation of the 1902–99 period. The PCs of the Trend, Pacific, and Atlantic modes are plotted as thin continuous, thick continuous, and dashed lines, respectively.

TABLE 1. Basic details of the models analyzed: acronym, horizontal and vertical resolutions of the atmospheric model, SST forcing and their references, period of integration, and the ensemble members available.

Model	Resolution	SST forcing	Period	Ensembles
CAM3.5	T85, L26	Improved HadISST and optimal interpolation (OIv2) SSTs; Hurrell et al. (2008)	1871–2006	1
CCM3	T42, L18	HadISST and Kaplan SSTs; (Rayner et al. 2003) and Kaplan et al. (1998)	1856–2007	16
NSIPP-1	3° lat × 3.75° lon, L34	HadISST; Rayner et al. (2003)	1902–2006	14

Links between precipitation variability over the central United States and adjoining SSTs are then obtained using the Hadley Centre's Sea Ice and SST (HadISST) analysis that spans the time period 1870–2002 on a 1° grid (Rayner et al. 2003), which is used on a coarser 5° × 2.5° grid.

It is necessary to mention the following working definitions. Unless noted otherwise, climatology and long-term variability in the twentieth century are obtained for the 1902–99 base period. To avoid intraseasonal variability, the basic data is seasonal and defined in terms of the typical three-month means: December–February for winter, March–May for spring, June–August for summer, and September–November for fall; thus, the data start in spring 1902 and ends in fall 1999.

Targets for the idealized simulations of precipitation are sought by regression of the principal components associated with the SST forcing patterns on observations and AMIP simulations. As mentioned in Schubert et al. (2009), the SST forcing comes from a rotated empirical orthogonal function (REOF) analysis, via the varimax rotation, of annual mean global SSTs for the period 1901–2004. These modes of SST variability are referred to as *Trend*, *Pacific*, and *Atlantic* forcing patterns (Figs. 1a–c). The associated rotated principal components (RPCs) are also shown here (Fig. 1d) but they have been standardized for the 1902–99 period. The Trend pattern shows a nonlinear long-term time evolution (thin continuous line). The Pacific pattern varies on both interannual (ENSO) and decadal time scales (thick continuous line). The Atlantic pattern also shows both decadal and interannual variations (thick dashed line), like those in the Atlantic multidecadal oscillation pattern (e.g., Enfield et al. 2001; Guan and Nigam 2009).

The cold Pacific idealized experiment from the three models is the only idealized simulation considered here. Differences between the seasonal precipitation climatologies of the idealized experiment and the control simulation (whose only forcing is the monthly SST climatology) will be contrasted against the regressed precipitation anomalies of the cold Pacific PC. The forcing for the cold Pacific experiment is obtained when the SST pattern of anomalies for the Pacific mode (Fig. 1b) are flipped in

sign. Likewise, regressions with the cold Pacific principal components (PCs) are obtained by flipping the signs of the Pacific PC (Fig. 1d).

3. Precipitation variability

The North American subcontinent experiences year-to-year hydroclimate variability. A simple way to portray that variability is by means of the standard deviation of seasonal precipitation. Maps in Fig. 2 display the standard deviation of summer precipitation in observations and AMIP simulations in the twentieth century. It is clear from the observations that the largest interannual variability of summer precipitation over the United States is over the central Great Plains, and along the Gulf of Mexico and Atlantic coasts. Comparable variability is also seen along western Mexico, that is, the Mexican portion of the North American monsoon region; however, the largest regional variability is along the eastern seaboard of Mexico.

Summer precipitation variability by the models is quasi-realistic. All models show low (high) variability in the western (eastern) half of United States, as well as large variability over western and southern Mexico. While all models have a maximum over the central United States that resembles the maximum in observations, the apparent connection with the Gulf coast states present in the observations is missing in the CAM3.5 and CCM3 models. The maximum values over the central United States in the CCM3 and NSIPP-1 models, shown by the mean standard deviation of their corresponding ensembles, are larger than in CAM3.5 and observations. This is a reflection of the fact that a large percentage of the individual ensemble simulations by those models tends to also have large variability (not shown). In fact, comparison of the summer standard deviation of the different ensemble members from CCM3 and NSIPP-1 models (not shown) indicates that the structure shown by the mean standard deviation is consistently similar in the individual ensembles, with a maximum over the central United States displaced to the west. While all models have muted variability over the eastern seaboard of the United States and Mexico, CAM3.5 is the only model that simulates the

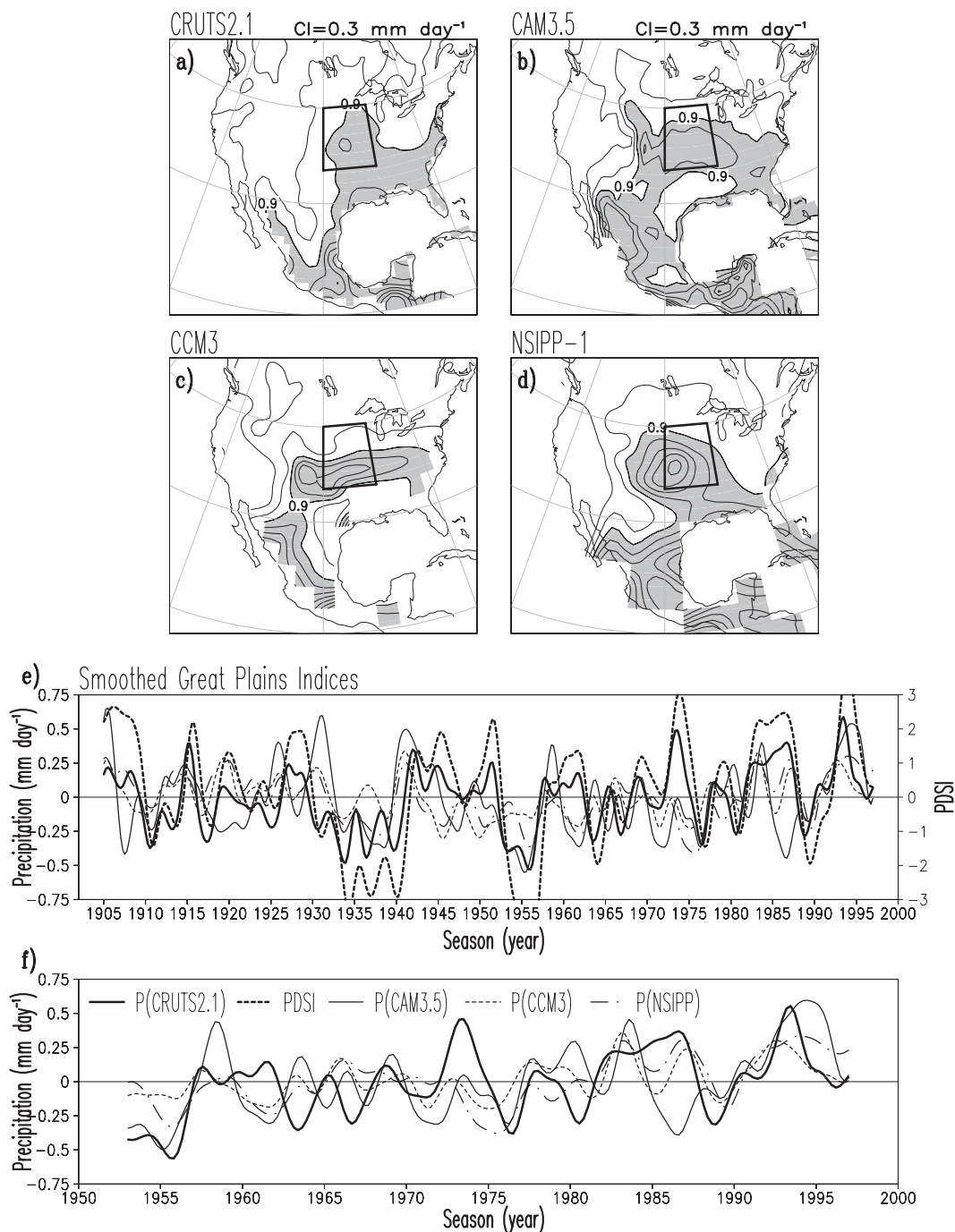


FIG. 2. Standard deviation of summer precipitation and seasonal precipitation indices in the twentieth century in the observations and AMIP simulations calculated for the period 1902–99: (a) CRUTS2.1, (b) CAM3.5, (c) CCM3 (mean of 16 ensembles), and (d) NSIPP-1 (mean of 14 ensembles). Contour interval is 0.3 mm day^{-1} and shading is for values $\geq 0.9 \text{ mm day}^{-1}$. The boxes in the different panels define the Great Plains region (35° – 45° N, 100° – 90° W) used to characterize the regional precipitation variability for the (e) 1902–99 and (f) 1950–99 periods. The indices for the period 1950–99 are displayed to highlight the increasing trend in the last part of the century. Indices have been smoothed via a 1–2–1 binomial index applied 12 times to seasonal anomalies for observations from CRUTS2.1 (thick continuous line) and PDSI (thick short-dashed line), CAM3.5 (continuous thin line), CCM3 (mean index from 16 ensembles: thin dashed line), and NSIPP-1 (mean index from 14 ensembles: thin dashed-dotted line).

TABLE 2. Correlations of the observed CRUTS2.1 smoothed Great Plains precipitation index with observed smoothed PDSI and the simulated smoothed precipitation indices for the 1902–99 period. The top row displays correlations for the smoothed raw indices, and the bottom row displays correlations for the smoothed, detrended indices. Precipitation indices for CCM3 and NSIPP-1 are mean indices from their 16- and 14-ensemble members, respectively.

CRUTS2.1	PDSI	CAM3.5	CCM3	NSIPP-1
Raw	0.84	0.30	0.23	0.39
Detrended	0.84	0.32	0.27	0.43

maximum over western Mexico, likely because of the finer resolution in this model.

Variability in the Great Plains

Precipitation variability in the central United States can be characterized by means of an index. The convenience of an index stems from the fact that this can help to establish local and remote connections and lead/lag relationships with other fields. An index that can contain the largest regional variability of summer precipitation in the central United States can be generated by area-averaging seasonal anomalies over the Great Plains region (35°–45°N, 100°–90°W); this region is outlined by a box in the maps in Fig. 2. In this way, seasonal Great Plains precipitation indices are defined for the observations and model simulations, as well as a Great Plains PDSI index for observations.

A frequent field used to monitor droughts is the PDSI, which is not a routine field for climate model simulations. However, a proxy to the PDSI can be obtained by smoothing seasonal precipitation anomalies. Thus, in order to create the proxy for PDSI and at the same time to focus on variability at interannual and longer time scales, the seasonal indices are smoothed by applying 12 times a 1–2–1 binomial filter. Doing so, correlation between the observed Great Plains precipitation and PDSI indices increases from 0.54 when the indices are not smoothed to 0.84 when both indices are smoothed. Thus, the smoothed precipitation index can be used as a proxy to the drought index in both observations and, more importantly, model simulations. Figure 2, also shows the smoothed observed and simulated Great Plains indices for the 1902–99 and 1950–99 periods. It is interesting to note that some major events are reasonably well captured by the simulations, for instance, the middle of the Dust Bowl, the droughts in the early 1950s and 1988, as well as the pluvial of 1993. However, correlations are not very high for the period 1902–99, in the 0.2–0.4 range, but increase for the shorter 1950–99 period, in the 0.4–0.5 range, as can be seen in Tables 2 and 3.

TABLE 3. As in Table 2, but for the 1950–99 period.

CRUTS2.1	PDSI	CAM3.5	CCM3	NSIPP-1
Raw	0.87	0.38	0.44	0.50
Detrended	0.83	0.20	0.28	0.31

The indices displayed in Fig. 2 show an increased trend that is particularly evident in the second half of the twentieth century. Thus, one can only wonder about the influence of the trend in the correlations. When the linear trend is extracted from the seasonal data, and then the smoothing is performed, the correlations are considerably reduced for the short period 1950–99, in the 0.2–0.3 range, and slightly increased for the long period 1902–99, in the 0.3–0.4 range, as can be seen in Tables 2 and 3. Thus, the linear trend present in the data is particularly influential in the second half of the twentieth century, and one should account for that in any analysis.

4. SST links to summer Great Plains precipitation

Hydroclimate variability over a region like the Great Plains can be remotely forced by SST anomalies. To explore this link in the observations, and model simulations in the warm season, a summer-only Great Plains index is extracted from the observed and simulated smoothed, detrended precipitation indices and then correlated with observed global, detrended, seasonal SST anomalies from the Hadley Centre dataset. In the case of the multiensemble CCM3 and NSIPP-1 models correlations are calculated for each ensemble and then a mean correlation map is obtained. Spread of the ensemble correlations is calculated by obtaining the standard deviation of the correlations in each model. Figure 3 displays those correlations for the period 1902–99. It is clear that the observed simultaneous summer correlations are modest, with the largest values of -0.3 over the subtropical Atlantic Ocean and 0.3 over the tropical Pacific Ocean; correlations over the Pacific Ocean show a coherent basin-scale structure of tropical–subtropical positive correlations and subtropical negative correlations resembling the Pacific decadal oscillation pattern. Maximum correlations are comparable in the Atlantic and Pacific Oceans. Weaker correlations are also present over the Indian Ocean as well. If the shorter period 1950–99 is used, the correlations increase especially over the midlatitude Pacific and Atlantic Oceans and decrease over the Indian Ocean (not shown). If the linear trend is kept in both the proxy drought index and the SST anomalies, correlations increase over the Indian Ocean, more so if the shorter period 1950–99 is used (not shown).

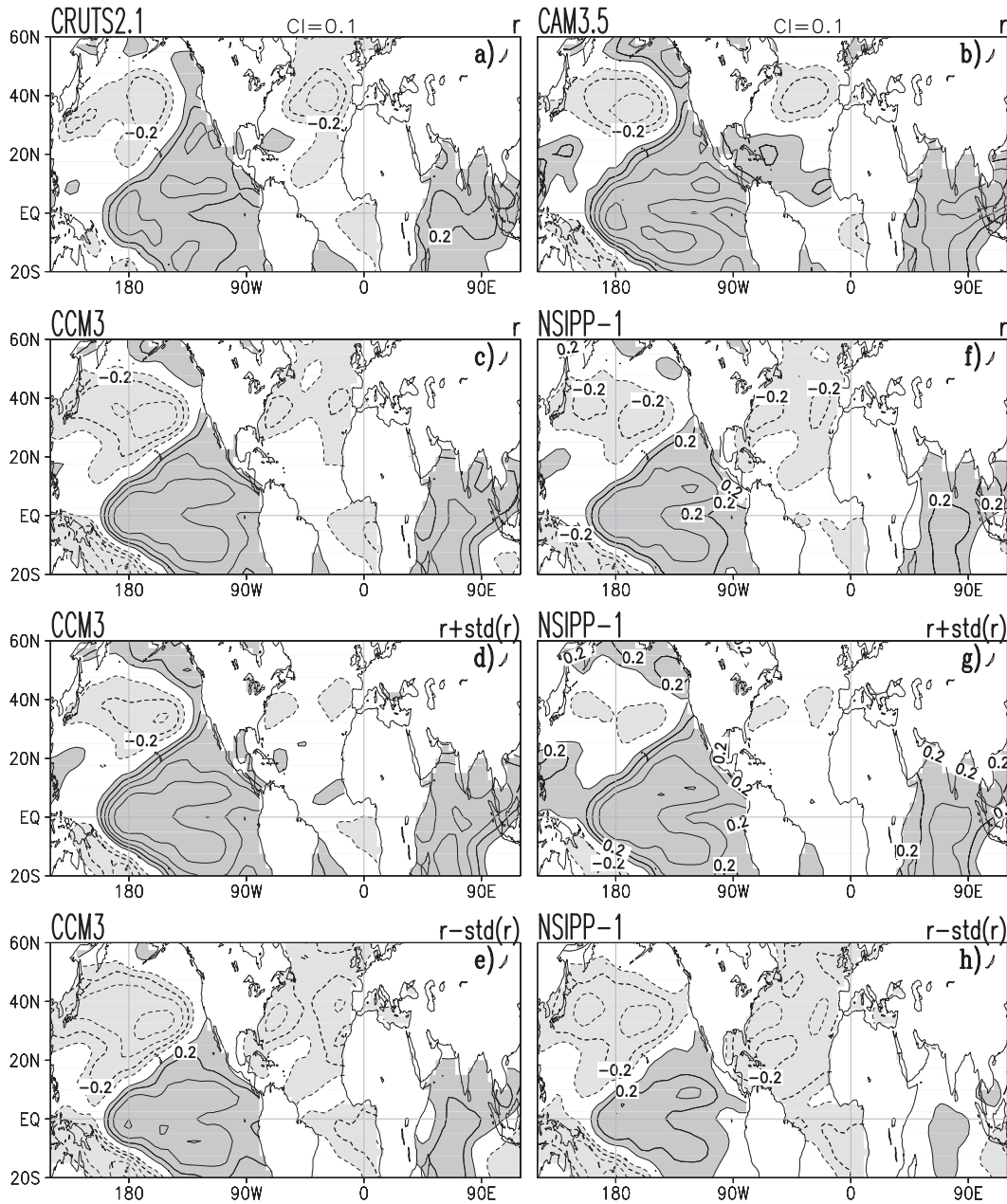


FIG. 3. SST correlations, r , with summer smoothed, detrended Great Plains precipitation indices from observations and AMIP simulations calculated for the period 1902–99: (a) CRUTS2.1, (b) CAM3.5, (c) CCM3 (mean from 16 ensembles), (d) CCM3 (mean correlation plus one standard deviation of correlations), (e) CCM3 (mean correlation minus one standard deviation of correlations), (f) NSIPP-1 (mean from 14 ensembles), (g) NSIPP-1 (mean correlation plus one standard deviation of correlations), and (h) NSIPP-1 (mean correlation minus one standard deviation of correlations). Seasonal SST anomalies, from the Hadley Centre’s Sea Ice and SST analysis, are detrended. Positive (negative) correlations are shaded dark (light); contour interval is 0.1. A two-tailed Student’s t test at the 0.05 level indicates significant correlations $\geq |\pm 0.21|$.

Models depict the correlation structure between the observed summer precipitation and SSTs. Correlations over the Pacific and Indian Oceans in the simulations are stronger than observations indicate, especially in the

single ensemble member from CAM3.5. Mean correlations with the multiensemble models CCM3 and NSIPP-1 are weaker than the single ensemble CAM3.5; NSIPP-1 shows the lowest correlations between summer precipitation

and SSTs. However, the spread of the correlations in the multiensemble models indicates that the structure may change from an almost nonexistent to a robust connection with the Atlantic. As in the case of observations, anomalies over the Indian Ocean are reduced for the shorter 1950–99 period but increase if the linear trend is kept (not shown).

It is interesting to point out that precipitation variability over the Great Plains in models like CAM3.5 and NSIPP-1 do have a SST connection very much like in observations.¹ However, the regional atmospheric water balance in those models shows a picture that is not consistent with observations. Local land surface–atmosphere interactions are the dominant influence over the external influence of the SSTs that drive moisture fluxes and moisture flux convergence over the region in those and some other models (Ruiz-Barradas and Nigam 2005, 2006b). Thus, the reading one has from these analyses is that the local effects in those models prevent them from a better simulation of precipitation variability over the central United States in the warm season.

The present precipitation-centric analysis shows that low-frequency summer precipitation variability in the observations and models has links with the neighboring oceans but it does not provide any insight on the separate roles of the oceans. Comparison with the main modes of annual-mean SST variability (Figs. 1b and 1c) shows some similarities with the structure of the oceanic footprint of the Great Plains precipitation variability, especially over the midlatitudes of the Pacific and Atlantic Oceans, and the Indian Ocean (Fig. 3). This suggests a possible role of the oceanic basins in generating precipitation variability over the central United States that is explored in the context of the main modes of annual SSTs used for the idealized experiments.

5. Precipitation evolution under imposed annual-mean SST anomalies

The idealized experiments by the DWG models do not have an observational counterpart or an observationally based target by the same models. A way to circumvent this absence of a target is by regressing the principal components associated with the Trend, Pacific, and Atlantic modes of annual-mean SSTs (Fig. 1d) on seasonal precipitation anomalies from observations and

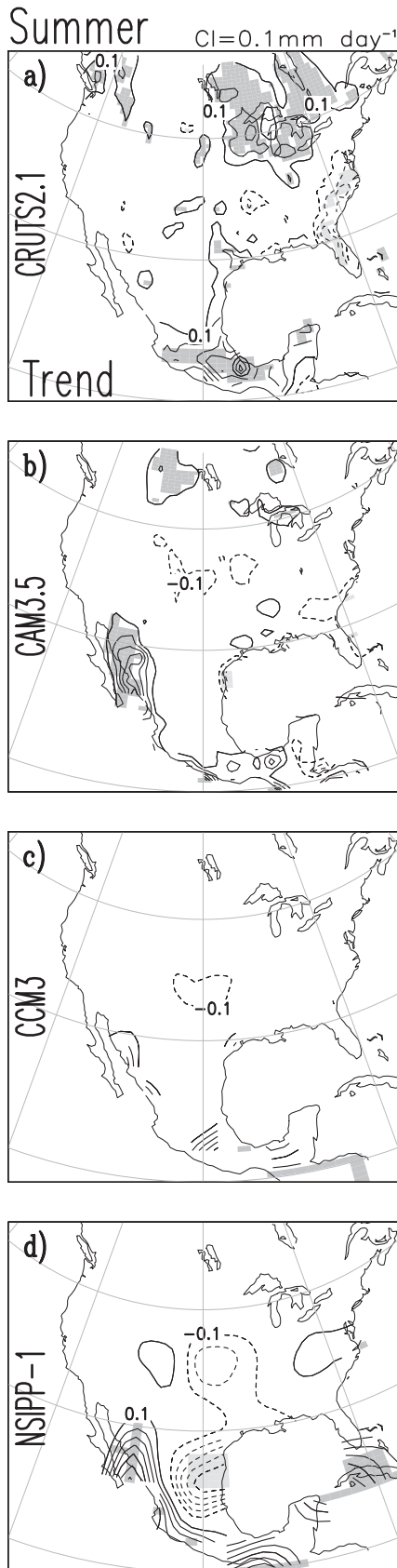
AMIP simulations. By imposing the PC value of a given year for a given season within that year, one can recognize the effect of the PC on the specific season in the regressed fields. Figures 4–6 display the seasonal regressions of the PCs corresponding to a warming Trend in summer, a cold Pacific from spring to fall, and a warm Atlantic in summer and fall, respectively, on the observed and simulated precipitation anomalies in the 1902–99 period. In the case of the multiensemble simulations by the CCM3 and NSIPP-1 models, the mean of the regressions is displayed for each model.

Summer precipitation under the nonlinear warming Trend influence (Fig. 4) shows some common results between observations and simulations. Observations indicate that Trend produces dry conditions over the central and eastern seaboard regions of the United States and pluvial conditions in the southern half of Mexico. While all models capture the dry conditions over the central United States, the drying of the eastern seaboard is partially captured by the CAM3.5 model. The broad structure of the pluvial conditions over southern Mexico is captured by all models.

The seasonal evolution of precipitation from spring to fall of the cold Pacific (Fig. 5) shows consistent results between observations and simulations, but differences are still evident. Observations indicate dry conditions over the U. S. Southwest and southern Great Plains emerging from the gulf states of Texas and Louisiana, but pluvial conditions over the eastern United States that weaken from spring to fall. The dry conditions move northward toward the central Great Plains, and the pluvial conditions move eastward in summer, and eventually the dry conditions reach the largest extension and magnitude over almost the whole eastern half of the United States in fall, with maximum values over the Great Plains. Pluvial conditions are also evident in the U.S. Northwest in fall as well as in southern Mexico, especially in summer and fall. While all models seem to capture the evolving dry conditions in the United States, they favor the largest deficit in precipitation in summer and not in fall as the observations indicate. Pluvial conditions over the U. S. Northwest in the models are fictitious in spring but not in fall. Common features in the models but not in observations include the subcontinental scale of the dry conditions in spring and the lack of pluvial conditions over the eastern United States. Pluvial conditions over southern Mexico in summer and fall are, on the other hand, captured by the models.

The seasonal evolution of precipitation from summer to fall of the warm Atlantic (Fig. 6) shows more discrepancies than consistencies between observations and simulations. Pluvial conditions emerge to the east of the central Great Plains in summer just to be completely

¹ Precipitation is the result of (or has components forced by) SSTs, local evapotranspiration, and everything else, so correlations with SSTs will be maximized because the correlations with the other precipitation components will be uncorrelated to SSTs. Thus, large correlations between precipitation and SSTs are the result of the direct link between SSTs and the precipitation component forced by them.



overrun by dry conditions in the fall that emerge from the gulf states of Texas and Louisiana in observations. Interestingly, this structure of dry conditions in fall is similar to the cold Pacific case. Dry conditions over the U. S. Southwest seem to emerge from northwestern Mexico in the summer. Pluvial conditions over the U. S. Northwest are present in fall, and similar conditions persist over southern Mexico in both summer and fall. Pluvial conditions over the eastern half of the United States in summer and its change to dry conditions in fall present in the observations are only captured by CAM3.5. The models also capture the dry summer conditions over the southwestern United States and northwestern Mexico, but CCM3 and NSIPP-1 models extend those conditions too far to the north, reaching the central United States. The dry conditions observed over the Great Plains in fall are only partially captured by CAM3.5. Pluvial conditions over the northwestern United States in fall in the observations are not captured but those over southern Mexico in both summer and fall are broadly captured by the models.

6. A proxy for the idealized experiments

The above regressions serve as more than targets for the idealized simulations: they are a “poor man’s” recourse to uncovering the model response to idealized SST forcing—at least a primary assessment of it. Clearly, not all of the idealized DGW experiments could be mimicked this way, for instance, the ones where SST forcing is confined in a subregion (like the tropics) of the whole pattern (shown in Figs. 1a–c). Even so, regression analysis on routinely generated AMIP simulations can provide a “lay of the land” before embarking on an elaborate (and often expensive) suite of model integrations.

This point is illustrated by comparing the precipitation anomalies from regressions of the cold Pacific PC (Fig. 5) with the drought modeling signal (i.e., the difference in climatological seasonal precipitation between the cold Pacific and control experiments) in Fig. 7. The control case experiment is run by imposing permanent monthly climatological SSTs as the only forcing to the models, while the cold Pacific case is run by superposing

FIG. 4. Simultaneous summer precipitation regressions on the PC of the Trend mode calculated for the period 1902–99: (a) CRUTS2.1, (b) CAM3.5, (c) CCM3 (mean from 16 ensembles), and (d) NSIPP-1 (mean from 14 ensembles). Statistically significant positive (negative) anomalies following a two-tailed Student’s *t* test at the 0.05 level are shaded dark (light); contour interval is 0.1 mm day⁻¹.

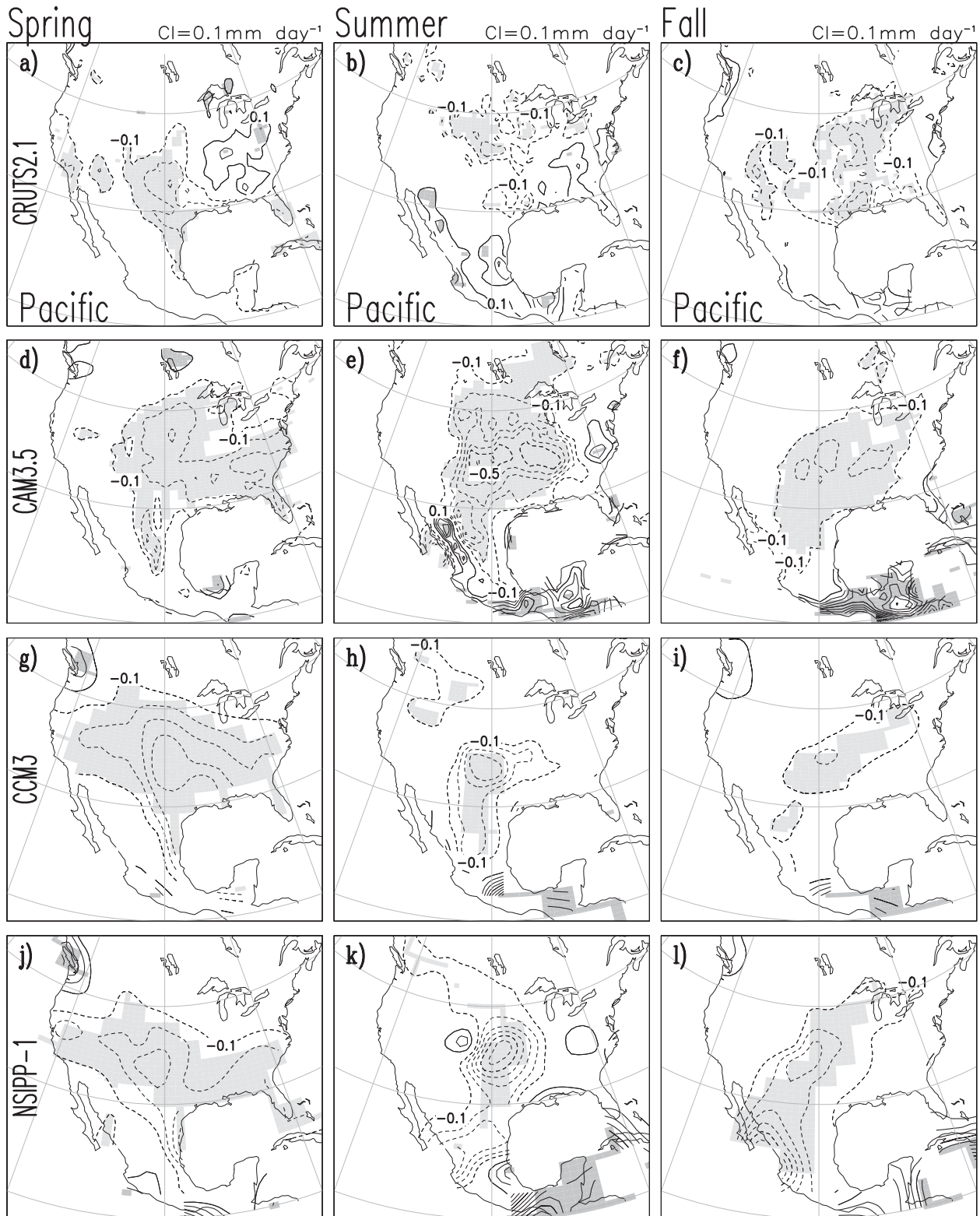


FIG. 5. Simultaneous seasonal precipitation regressions on the PC of the Pacific mode calculated for the period 1902–99 for (left) spring, (middle) summer, and (right) fall regressions: (a)–(c) CRUTS2.1, (d)–(f) CAM3.5, (g)–(i) CCM3 (mean from 16 ensembles), and (j)–(l) NSIPP-1 (mean from 14 ensembles). Statistically significant positive (negative) anomalies following a two-tail Student's t test at the 0.05 level are shaded dark (light); contour interval is 0.1 mm day^{-1} .

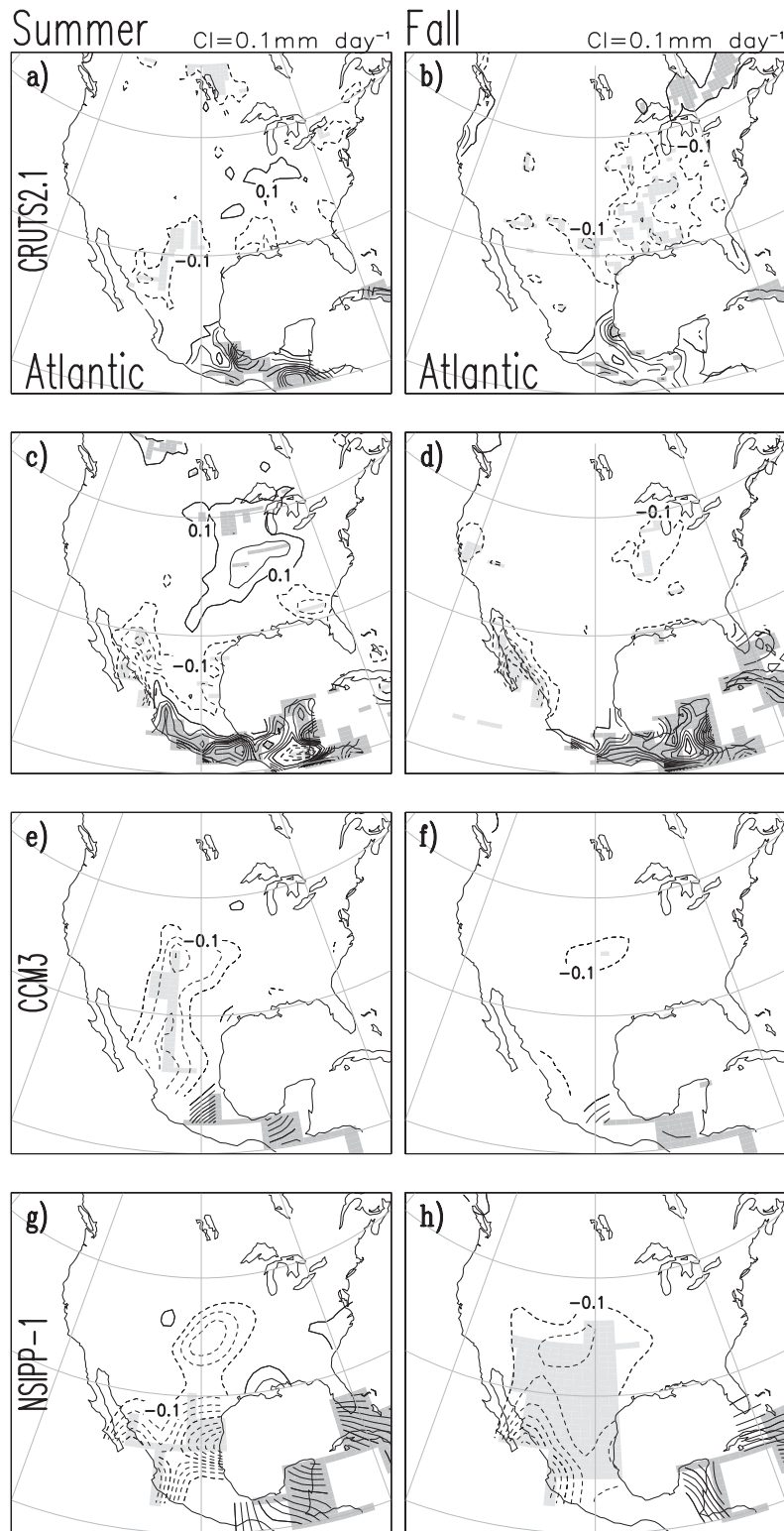


FIG. 6. As in Fig. 5, but of the Atlantic mode for (left) summer and (right) fall.

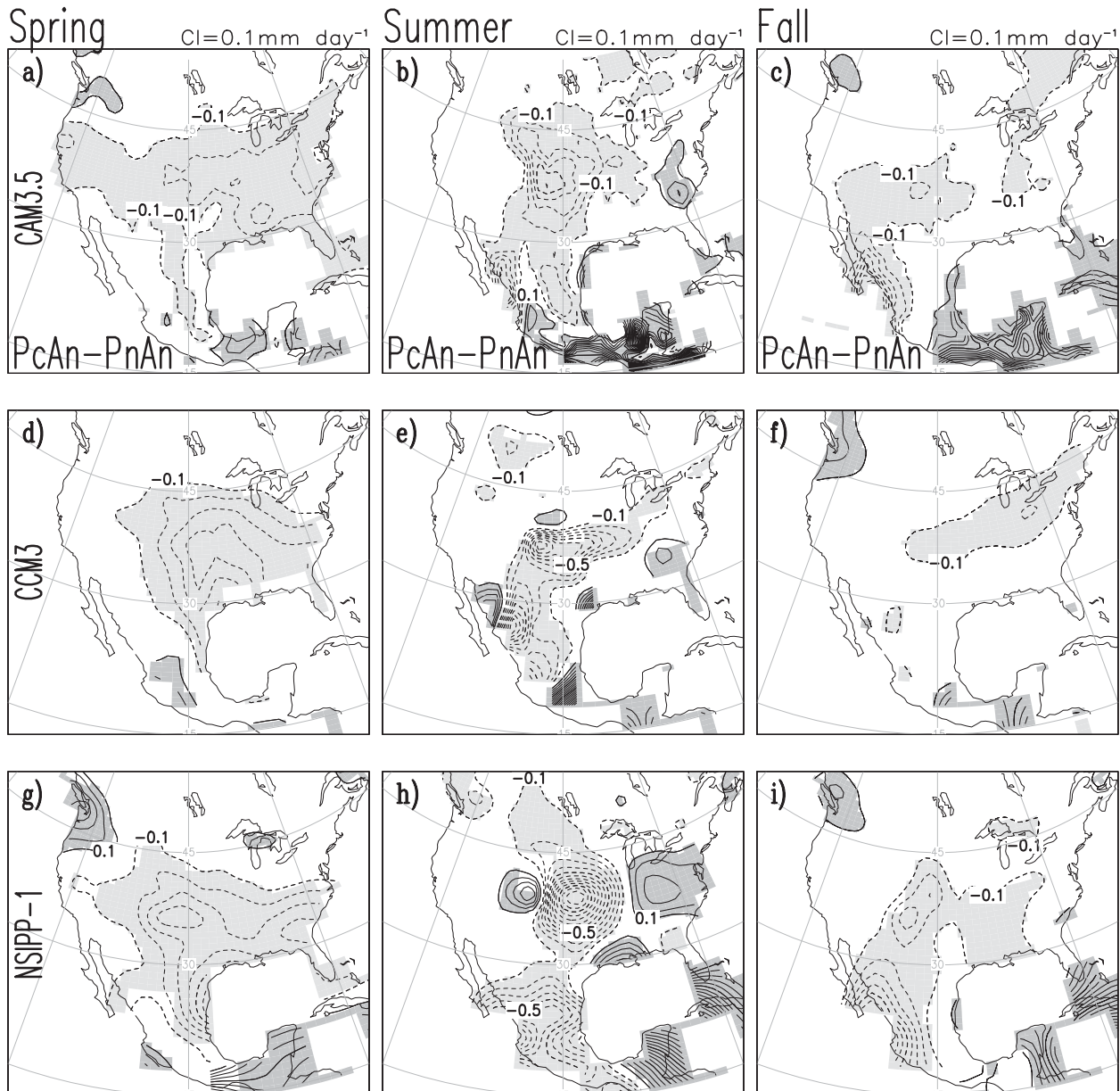


FIG. 7. Climatological seasonal precipitation differences obtained from the cold Pacific-only, 50-yr idealized experiment for (left) spring, (middle) summer, and (right) fall regressions: (a)–(c) CAM3.5, (d)–(f) CCM3, and (g)–(i) NSIPP-1. The forcing in this simulation is the time-invariant cold Pacific SST pattern (anomalies in Fig. 1b are flipped in sign) superposed onto the monthly climatological SSTs. Climatological seasonal differences are with respect to the control simulation forced with global varying monthly climatological SSTs. Differences have been divided by 2. Statistically significant positive (negative) differences following a two-tail student's t test at the 0.05 level are shaded dark (light); contour interval is 0.1 mm day^{-1} .

the time-invariant negative phase of the Pacific pattern (Fig. 1b) onto the climatological monthly SSTs.

The anomaly structure in the cold Pacific experiment is very similar to that obtained from regressions of the cold Pacific PC. The large magnitude in the precipitation anomalies from the idealized experiment arises as a consequence of the strong forcing imposed in the models

(Schubert et al. 2009) and its permanent imposition throughout the year. Common to both sets of figures are the evolving dry conditions over the central United States, which are already large in spring, peak in summer, and decay notably in fall. Pluvial conditions over southern Mexico in summer and fall are also common features in regressions and idealized experiments.

The idealized warm Atlantic drought modeling experiment can also be mimicked by precipitation regressions of the related SST principal component, although not to the extent of the cold Pacific SST pattern. The Atlantic principal component regressions (not shown) are weaker than those from the cold Pacific forcing. Widespread precipitation anomalies over the United States in the idealized modeling experiment with a warm Atlantic are not present in the regressions. However, dry (wet) anomalies over the western (eastern) half of Mexico are present in both the idealized experiment and regressions.

Regression analysis of AMIP simulations can be very insightful. The observed SST forcing in the AMIP simulations provides them with a rich structure variability, which is often sufficient for discerning the related model's response to prescribed SST anomalies, including idealized ones, as shown above. Clearly, such analysis must constitute the pilot phase of a more elaborate (and expensive) modeling program.

7. Concluding remarks

The present study has as a goal the evaluation of the ability of the models of the DWG to simulate low-frequency summer precipitation variability over North America in general, and over the Great Plains in particular. Two issues of fundamental interest in this analysis are to find 1) common SST structures that may be driving low-frequency summer hydroclimate variability over the central United States in observations and simulations and 2) analogs in observations and simulations that allow assessment of the idealized drought experiments carried out by the DWG models. The main findings are summarized.

- Differences exist in the distribution of the standard deviation of summer precipitation. Models tend to displace the center of maximum variability westward over the central United States. Among the models with multiensemble simulations, NSIPP-1 has the largest variability, while CCM3 has the smallest variability.
- There is a modest skill in simulating low-frequency variability of precipitation, or its proxy, the PDSI, that is useful for model simulations, over the central Great Plains. Correlations are in the 0.2–0.4 range for the 1902–99 record, but increase to 0.4–0.5 for the 1950–99 record.
- There is a linear trend component implicit in the central Great Plains precipitation variability, particularly evident in the second half of the twentieth century. Trend-removed correlations marginally increase in the 1902–99 record, but they decrease to the 0.2–0.3 range in the 1950–99 record.
- Detrended summer SST links of the Great Plains proxy drought index in the observations and model simulations show connectivity with both Pacific and Atlantic Oceans. The dominant structure over the Pacific has features resembling the Pacific decadal oscillation pattern; secondary features of opposite sign are over the midlatitude Atlantic Ocean. These features are independent of the trend or period used.
- Precipitation variability over the United States associated with the PCs of the warm Trend, cold Pacific, and warm Atlantic modes of annual-mean SSTs have a preferred seasonality and spatial focus. Observations indicate that the warm Trend, cold Pacific, and warm Atlantic modes consistently affect the U. S. Southwest, Midwest, and U. S. Southeast regions, with the Great Plains always stressed by the deficit of precipitation.
- AMIP simulations indicate that the seasonal precipitation responses to the warm Trend, cold Pacific, and warm Atlantic modes in the models capture broad features from observations but inconsistencies remain to be solved, especially in the seasonality.
- AMIP simulations can be used as a proxy for more elaborate idealized experiments. This baseline analysis provides some guidance for future modeling experiments.

Acknowledgments. This work was carried out as part of a U.S. CLIVAR Drought Working Group activity supported by NASA, NOAA, and NSF to coordinate and compare climate model simulations forced with a common set of idealized SST patterns. The authors thank NASA's Global Modeling and Assimilation Office (GMAO) for making the NSIPP1 runs available, the Lamont-Doherty Earth Observatory of Columbia University for making their CCM3 runs available, NOAA's Climate Prediction Center (CPC)/Climate Test Bed (CTB) for making the GFS runs available, NOAA's Geophysical Fluid Dynamics Laboratory (GFDL) for making the AM2.1 runs available, the National Center for Atmospheric Research (NCAR) for making the CAM3.5 runs available, and the Center for Ocean–Land–Atmosphere (COLA) and the University of Miami's Rosenstiel School of Marine and Atmospheric Science for making the CCSM3.0 coupled model runs available. The authors wish to acknowledge support from NOAA CPPA Grant NA17EC1483, and NSF Grants DRICOMP ATM0738907 and ATM0649666, as well as DOE Grant DEFG0208ER64548. The authors would also like to thank two anonymous reviewers for their constructive comments that helped to improve the quality of this paper.

REFERENCES

- Bacmeister, J., P. J. Pegion, S. D. Schubert, and M. J. Suarez, 2000: An atlas of seasonal means simulated by the NSIPP 1 atmospheric GCM. NASA Tech. Memo. 104606, Vol. 17, Goddard Space Flight Center, Greenbelt, MD, 194 pp.
- Barlow, M., S. Nigam, and E. H. Berbery, 2001: ENSO, Pacific decadal variability, and U.S. summertime precipitation, drought, and stream flow. *J. Climate*, **14**, 2105–2128.
- Campana, K., and P. Caplan, Eds., cited 2009: Technical procedure bulletin for T382 Global Forecast System. [Available online at http://www.emc.ncep.noaa.gov/gc_wmb/Documentation/TPBoct05/T382.TPB.FINAL.htm.]
- Dai, A., K. E. Trenberth, and T. Qian, 2004: A global data set of Palmer drought severity index for 1870–2002: Relationship with soil moisture and effects of surface warming. *J. Hydro-meteor.*, **5**, 1117–1130.
- Delworth, T. L., and Coauthors, 2006: GFDL's CM2 global coupled climate models. Part I: Formulation and simulation characteristics. *J. Climate*, **19**, 643–674.
- Enfield, D., A. Mestas-Núñez, and P. Trimble, 2001: The Atlantic multidecadal oscillation and its relation to rainfall and river flows in the continental U.S. *Geophys. Res. Lett.*, **28**, 2077–2080.
- Guan, B., and S. Nigam, 2009: Analysis of Atlantic SST variability factoring interbasin links and the secular trend: Clarified structure of the Atlantic multidecadal oscillation. *J. Climate*, **22**, 4228–4240.
- Gutzler, D., and S. Schubert, 2007: The U.S. CLIVAR Working Group on long-term drought. *U.S. CLIVAR Variations*, Vol. 5, No. 1, U.S. CLIVAR Office, Washington, DC, 6–7.
- Hurrell, J. W., J. J. Hack, D. Shea, J. M. Caron, and J. Rosinski, 2008: A new sea surface temperature and sea ice boundary data set for the Community Atmosphere Model. *J. Climate*, **21**, 5145–5153.
- Kaplan, A., M. A. Cane, Y. Kushnir, A. C. Clement, M. B. Blumenthal, and B. Rajagopalan, 1998: Analyses of global sea surface temperature: 1856–1991. *J. Geophys. Res.*, **103**, 18 567–18 589.
- Kiehl, J. T., J. J. Hack, G. Bonan, B. A. Boville, D. Williamson, and P. Rasch, 1998: The National Center for Atmospheric Research Community Climate Model: CCM3. *J. Climate*, **11**, 1131–1149.
- Mitchell, T. D., 2005: An improved method of constructing a database of monthly climate observations and associated high resolution grids. *Int. J. Climatol.*, **25**, 693–712.
- Neale, R. B., J. H. Richter, and M. Jochum, 2008: The impact of convection on ENSO: From a delayed oscillator to a series of events. *J. Climate*, **21**, 5904–5924.
- Oleson, K. W., and Coauthors, 2008: Improvements to the Community Land Model and their impact on the hydrological cycle. *J. Geophys. Res.*, **113**, G01021, doi:10.1029/2007JG000563.
- Rayner, N. A., D. E. Parker, E. B. Horton, C. K. Folland, L. V. Alexander, D. P. Rowell, E. C. Kent, and A. Kaplan, 2003: Global analyses of sea surface temperature, sea ice, and night marine air temperature since the late nineteenth century. *J. Geophys. Res.*, **108**, 4407, doi:10.1029/2002JD002670.
- Ruiz-Barradas, A., and S. Nigam, 2005: Warm-season precipitation variability over the U.S. Great Plains in observations, NCEP and ERA-40 reanalyses, and NCAR and NASA atmospheric simulations. *J. Climate*, **18**, 1808–1830.
- , and —, 2006a: Great Plains hydroclimate variability: The view from North American Regional Reanalysis. *J. Climate*, **19**, 3004–3010.
- , and —, 2006b: IPCC's twentieth-century climate simulations: Varied representations of North American hydroclimate variability. *J. Climate*, **19**, 4041–4058.
- Schubert, S. D., M. J. Suarez, P. J. Pegion, R. D. Koster, and J. T. Bacmeister, 2004: Causes of long-term drought in the U.S. Great Plains. *J. Climate*, **17**, 485–503.
- , and Coauthors, 2009: A U.S. CLIVAR project to assess and compare the responses of global climate models to drought-related SST forcing patterns: Overview and results. *J. Climate*, **22**, 5251–5272.
- Seager, R., Y. Kushnir, C. Herweijer, N. Naik, and J. Velez, 2005: Modeling tropical forcing of persistent droughts and pluvials: 1856–2000. *J. Climate*, **18**, 4068–4091.
- Ting, M., and H. Wang, 1997: Summertime U.S. precipitation variability and its relation to Pacific sea surface temperature. *J. Climate*, **10**, 1853–1873.
- Trenberth, K. E., and C. J. Guillemot, 1996: Physical processes involved in the 1988 and 1993 floods in North America. *J. Climate*, **9**, 1288–1298.
- Weaver, S. J., and S. Nigam, 2008: Variability of the Great Plains low-level jet: Large-scale circulation context and hydroclimate impacts. *J. Climate*, **21**, 1532–1551.